Organic & Biomolecular Chemistry

PAPER

View Article Online
View Journal | View Issue

Open Access Article. Published on 14 June 2019. Downloaded on 11/6/2025 9:33:02 PM.
This article is licensed under a Creative Commons Attribution-NonCommercial 3.0 Unported Licence.

Check for updates

Cite this: *Org. Biomol. Chem.*, 2019, **17**, 6404

Structural flexibility *versus* rigidity of the aromatic unit of DNA ligands: binding of aza- and azoniastilbene derivatives to duplex and quadruplex DNA†

H. Ihmels,* M. Karbasiyoun, K. Löhl and C. Stremmel‡

The known azastilbene (*E*)-1,2-di(quinolin-3-yl)ethane (**2a**) and the novel azoniastilbene derivatives (*E*)-2-(2-(naphthalen-2-yl)vinyl)quinolizinium (**2b**) and (*E*)-3,3′-(ethane-1,2-diyl)bis(1-methylquinolinin-1-ium) (**2c**) were synthesized. Their interactions with duplex and quadruplex DNA (G4-DNA) were studied by photometric, fluorimetric, polarimetric and *flow*-LD analysis, and by thermal DNA denaturation studies, as well as by ^{1}H-NMR spectroscopy. The main goal of this study was a comparison of these conformationally flexible compounds with the known G4-DNA-binding diazoniadibenzo[*b*,*k*]chrysenes, that have a comparable π-system extent, but a rigid structure. We have observed that the aza- and azoniastilbene derivatives **2a–c**, *i.e.* compounds with almost the same spatial dimensions and steric demand, bind to DNA with an affinity and selectivity that depends significantly on the number of positive charges. Whereas the charge neutral derivative **2a** binds unspecifically to the DNA backbone of duplex DNA, the ionic compounds **2b** and **2c** are typical DNA intercalators. Notably, the bis-quinolinium derivative **2c** binds to G4-DNA with moderate affinity (K_b = 4.8 × 10^5 M^{-1}) and also stabilizes the G4-DNA towards thermal denaturation (ΔT_m = 11 °C at ligand–DNA ratio = 5.0). Strikingly, the corresponding rigid counterpart, 4a,12a-diazonia-8,16-dimethyldibenzo[*b*,*k*]chrysene, stabilizes the G4-DNA to an even greater extent under identical conditions (ΔT_m = 27 °C). These results indicate that the increased flexibility of a G4-DNA ligand does not necessarily lead to stronger interactions with the G4-DNA as compared with rigid ligands that have essentially the same size and π system extent.

Received 8th April 2019,
Accepted 14th June 2019

DOI: 10.1039/c9ob00809h

rsc.li/obc

Introduction

Among the non-canonical DNA forms, the quadruplex DNA (G4-DNA), that is formed in G-rich DNA sequences upon stacking of at least two guanine quartets, is currently attracting most attention.[1] Thus, several G-rich DNA sequences with the propensity to fold into quadruplex structures have been identified in genomic nucleic acids,[2] for example in telomeric DNA and some promoter regions of oncogenes.[3] Moreover, it has been shown that some biologically relevant processes are directly related to quadruplex-DNA formation, such as the suppression of gene expression,[4] or the induction of the cellular response to DNA damage.[5] As a result of the essential biological functionality of quadruplex DNA, the association of an exogenous ligand with G4-DNA structures may have a significant effect on the biological function of G-rich DNA sequences, either by simply blocking the binding site of enzymes, which leads to their inhibition, or by increasing the thermodynamic stability and the lifetime of the G4-DNA.[1,6] In the latter case, enzyme inhibition may also occur when the enzyme requires the unwound form of the particular DNA sequence. Based on this principle, numerous G4-DNA-targeting molecules have been developed that may affect the biological activity of the DNA.[7] Along these lines, traditional DNA intercalators, *i.e.* cationic, planar, polycyclic (het)arenes, figure as a promising basis for the development of G4-DNA ligands. Thus, it has been shown that such intercalators have the propensity for a terminal π-stacking at the ends of G4-DNA structures.[1,7] Such as intercalation of a ligand between base pairs in duplex DNA,[8] the terminal π-stacking is driven by dispersion interactions between the aromatic ligand and the guanine quartet and by an additional hydrophobic effect as the lipophilic ligand migrates from the aqueous solution into the hydrophobic binding site.[9] Because of the thermodynamically

Department of Chemistry and Biology, University of Siegen, Adolf-Reichwein-Str. 2, 57068 Siegen, Germany. E-mail: ihmels@chemie.uni-siegen.de

† Electronic supplementary information (ESI) available: Absorption and emission data of **2a–c**; thermal DNA denaturation analysis; NMR spectra. See DOI: 10.1039/c9ob00809h

‡ Author names are in alphabetical order that does not reflect the specific contribution of each author.

This journal is © The Royal Society of Chemistry 2019

Open Access Article. Published on 14 June 2019. Downloaded on 11/6/2025 9:33:02 PM.
This article is licensed under a Creative Commons Attribution-NonCommercial 3.0 Unported Licence.

unfavorable process of the unwinding and disassembly of the quadruplex structure, planar aromatic ligands do usually not intercalate into G4-DNA. In this context, highly selective aromatic ligands have been developed that bind to the terminal end of the quadruplex due to their extended π-system, but whose structure does no longer allow a thermodynamically favorable intercalation into duplex DNA.[1a,b,7] In this context, we have shown that polycyclic azoniahetarenes, for example the diazoniadibenzo[*b*,*k*]chrysenes (**1a–c**), bind to G4-DNA even in the absence of additional functional side chains, thus enabling the assessment of the intrinsic ligand properties.[10] The binding modes of **1a–c** were studied in detail and all experimental data indicate the terminal π-stacking of the diazoniachrysenes to quadruplex DNA as the major binding mode. Thus, the size and topology of the π-systems of the cationic hetarenes **1a–c** enable sufficient overlap with the G-quartet mainly based on attractive π-stacking interactions.[10] It should be noted, however, that this class of quadruplex ligands consists of highly rigid compounds that have essentially no conformational flexibility. At the same time, some of the most promising and efficient G4-DNA ligands, such as *e.g.* the bis(quinolinium)pyridine dicarboxamides,[11] contain structural elements that provide a significant degree of conformational freedom, as the aromatic units are not completely annelated but connected by flexible linkers. It may be assumed that this structural flexibility facilitates the access of the ligand as well as the fit of the aromatic scaffold to the steric demand of the binding site. Along these lines, the influence of the structural flexibility of G4-DNA ligands has been shown recently by a comparison of structurally resembling flexible and rigid bis(quinolinium)-bisindole dicarboxamide derivatives.[12] In these ligands, the bisindole core unit, that is involved in the terminal π stacking to G4-DNA, is either connected in a flexible biaryl structure or kept rigid in a completely fused structure. It has been shown that these flexible derivatives have a slightly higher affinity to G4-DNA than the rigid ones because of the better ability of the flexible ligands to adapt to the G4-DNA structure. It should be noted, however, that even the rigid ligands in this study still contained flexible elements as the two quinolinium units were attached to the bisindole core through amide bonds that allow torsional movement. Before this background, we proposed that ligands with a similarly extended π-system as the dibenzochrysene derivatives **1a–c**, but with an increased conformational flexibility may have an increased affinity to G4-DNA. We identified the aza- and azoniastilbene derivatives **2a–c** as a promising starting point to check this proposal because they have a similarly extended π-system as **1a–c**, but more conformational flexibility due to the possible rotation about the aryl–alkene single bond. We proposed that these compounds bind to DNA as it has been shown already that pyridinium-based azoniastilbenes bind to DNA.[13] And more recently, it has been demonstrated that substituted styryl-quinolinium derivatives bind to G4-DNA.[14] Herein, we present the synthesis of stilbene derivatives **2a–c** and the investigation of their DNA-binding properties. For better comparison with respect to size and shape, we also synthesized and investigated the dimethyldiazoniadibenzo–chrysene **1d** in this study, because this derivative has methyl substituents at positions that correspond to the ones in the dimethyl-bis(quinolinium) derivative **2c**.

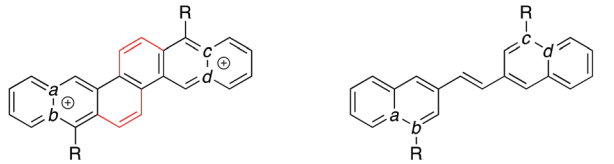

1a: *a* = *d* = N; *b* = *c* = C, R = H
1b: *b* = *c* = N; *a* = *d* = C, R = H
1c: *a* = *c* = N; *b* = *d* = C, R = H
1d: *a* = *d* = N; *b* = *c* = C, R = CH_3

2b: *a* = *b* = *c* = C, *d* = N^+, R = H
2c: *a* = *d* = C, *b* = *c* = N^+, R = CH_3

Results

Synthesis

The (*E*)-1,2-di(quinolin-3-yl)ethane (**2a**) was prepared according to published procedure[15] and subsequently quaternized by reaction with methyl iodide at high pressure[10a] to give the (*E*)-3,3′-(ethane-1,2-diyl)bis(1-methyl quinolinin-1-ium) (**2c**) in 70% yield (Scheme 1). The (*E*)-2-(2-(naphthalen-2-yl)vinyl) quinolizinium (**2b**) was synthesized in 62% yield by the base-catalyzed Knoevenagel-type reaction of 2-methylquinolizinium (**3**)[10b] with 2-naphthaldehyde (**4**) (Scheme 1).[10b,c] The dibenzochrysene derivative **1d** was synthesized starting from the reaction of 1,5-di(bromomethyl)naphthalene (**5**)[11] with 2-(2-methyl-(1,3)-dioxolan-2-yl)pyridine (**6**)[13] and subsequent ion metathesis to give bis(pyridiniummethyl)naphthalene **7**. The latter was treated with polyphosphoric acid (PPA) at 150 °C to give the cyclodehydration product **1d** in 75% yield (Scheme 2).

Absorption and emission properties

The absorption and emission spectra of the aza- and azoniastilbene derivatives **2a–c** were recorded in DMSO, MeCN, MeOH, water, and BPE buffer solution (Fig. 1, Table S1 in ESI†). The corresponding shifts and the band structures do not depend strongly on the solvent properties. Thus, the long-wavelength absorption maxima are lying in a rather small range of 325–333 nm (**2a**), 379–396 nm (**2b**) and 366–369 nm (**2c**), respectively. Likewise, most of the emission bands of each compound cover the same wavelength range with small Stokes shifts and low to moderate emission quantum yields (**2a**: λ_{fl} = 397–420 nm, Φ_{fl} = 0.2–0.5; **2b**: λ_{fl} = 491–499 nm, Φ_{fl} = 0.2; **2c**:

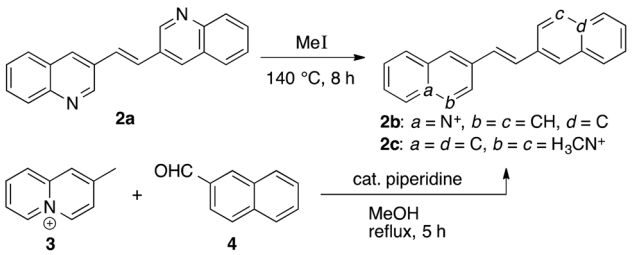

Scheme 1 Synthesis of stilbene derivatives **2b** and **2c**.

Open Access Article. Published on 14 June 2019. Downloaded on 11/6/2025 9:33:02 PM.
This article is licensed under a Creative Commons Attribution-NonCommercial 3.0 Unported Licence.

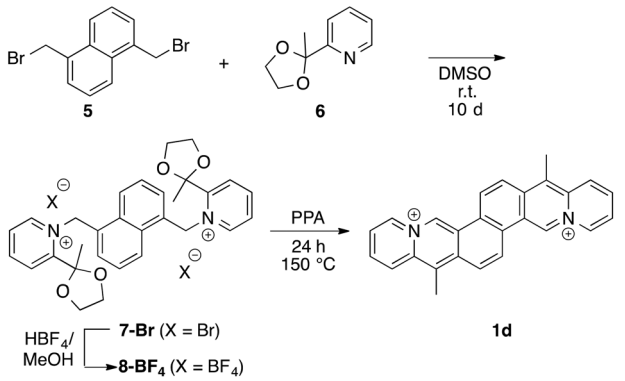

Scheme 2 Synthesis of 4a,12a-diazonia-8,16-dimethyldibenzo[*b*,*k*]chrysene (**1d**).

λ_{fl} = 454–462 nm Φ_{fl} = <0.01–0.3). As the only exception, the emission spectra of derivative **2a** in water and MeOH deviate from the ones in the other solvents; namely the bands are significantly broader with a very pronounced red-shifted shoulder (Fig. 1A), presumably indicating aggregation.

Spectrometric titrations with ct DNA

The interactions of the stilbene derivatives **2a–c** with double-stranded calf thymus (ct) DNA were monitored by photometric and fluorimetric titrations (Fig. 2). The absorption of derivative **2a** decreased during titration with no significant shift of the absorption maximum at 329 nm (Fig. 2A1). In the case of ligands **2b** and **2c**, the absorption maxima at 382 nm (**2b**) and 366 nm (**2c**) also decreased on addition of up to 2.8 (**2b**) and 6.1 (**2c**) molar equivalents of ct DNA, respectively, without shift of the maxima (Fig. 2A2 and A3). On further addition of DNA the absorption increased with a bathochromic shift of approx. 7 nm in each case. It should be noted that samples of **2b** were occasionally contaminated with traces of the photodimer whose formation is indicated by a weak absorption at 333 nm. In general, the characteristic emission of the stilbene derivatives **2a–c** was quenched on addition of ct DNA, which was accompanied in some cases by slight shifts of the emission maxima (Fig. 2B1–B3). In the case of ligand **2b**, a very small fluorescence light-up effect was observed in the first titration steps (molar equivalent <1) before the quenching occurs. The data from the photometric or fluorimetric titrations were plotted as binding isotherms and analyzed based on the theoretical binding model (*cf.* ESI†).[16] The resulting binding constants are 6.2 × 10^4 M^{-1} (**2a**), 5.1 × 10^4 M^{-1} (**2b**), and 2.0 × 10^5 M^{-1} (**2c**).

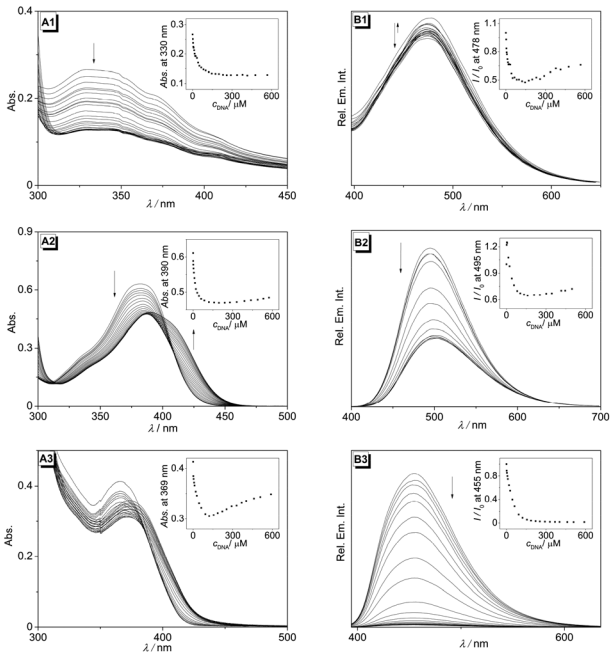

Fig. 2 Photometric (A) and fluorimetric titration (B); **2a**: λ_{ex} = 384 nm, **2b**: λ_{ex} = 342 nm, **2c**: λ_{ex} = 383 nm of ligands **2a** (1), **2b** (2) and **2c** (3) (*c* = 20 μM) with ct DNA (*c* = 1.0 mM in base pairs) in BPE buffer (pH = 7.0; **2a–b**: with 5% v/v DMSO); *T* = 20 °C. The arrows indicate the development of the absorption or emission bands during titration. Inset: Plot of absorption Abs/Abs_0 and relative emission I/I_0, resp., *versus* c_{DNA}.

Polarimetric titrations with ct DNA

To gain further insight into the DNA-binding modes the interactions between the ligands **2a–c** with ct DNA were examined by circular dichroism (CD) and flow linear dichroism (LD) spectroscopy (Fig. 3). Upon addition of DNA the compound **2a** developed a significant positive induced CD (ICD) band at 344 nm and negative ICD bands at 417 nm and 307 nm, but the latter was only observed at ligand–DNA-ratio (LDR) = 0.5 and 1.0. At the same time, the characteristic positive CD band of the DNA at 277 nm fluctuated slightly with increasing LDR values. In addition, *flow*-LD measurements revealed a developing positive signal in the absorption range of the ligand **2a**

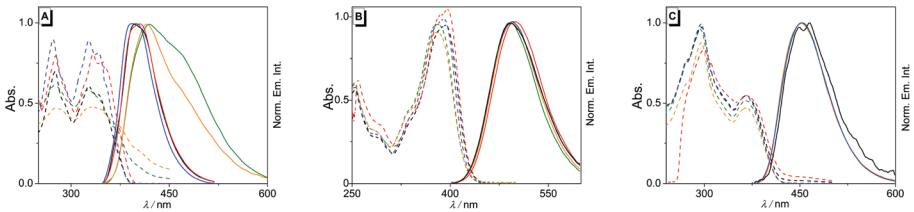

Fig. 1 Absorption (dashed lines; *c* = 25 μM) and emission spectra [continuous lines; **2a**: λ_{ex} = 334 nm, **2b**: 390 nm, **2c**: 320 nm of compounds **2a** (A), **2b** (B), and **2c** (C) in DMSO (red), MeCN (blue), water (green **2a**: with 5% DMSO), MeOH (black), and phosphate buffer (orange, **2a**: with 5% DMSO)].

Open Access Article. Published on 14 June 2019. Downloaded on 11/6/2025 9:33:02 PM.
This article is licensed under a Creative Commons Attribution-NonCommercial 3.0 Unported Licence.

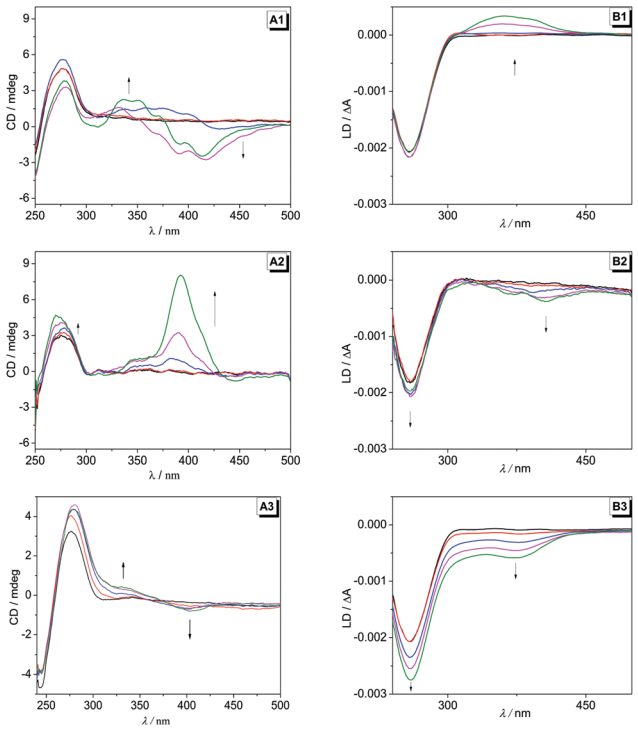

Fig. 3 CD (A) and *flow*-LD (B) spectra of mixtures of ligands **2a–c** and ct DNA in BPE buffer (pH = 7.00; **2a,b**: with 5% v/v DMSO) and at LDR 0.0 (black), 0.1 (red), 0.2 (blue), 0.5 (magenta) and 1.0 (green); c_{DNA} = 20 μM; T = 20 °C. Arrows indicate the development of CD and LD bands with increasing LDR value.

with a maximum at 361 nm (Fig. 3B1). The addition of DNA to a solution of compound **2b** induced the formation of positive ICD bands at 386 nm and 340 nm with relatively high intensity at large LDR. The complementary LD-spectroscopic experiments showed a weak negative LD band at 403 and 369 nm whose intensity increased slightly with increasing LDR. The addition of DNA to compound **2c** led to the formation of relatively weak positive and negative ICD bands at 332 nm and 405 nm (Fig. 3A3). The *flow*-LD measurements showed a developing negative LD band in the absorption range of the ligand with a maximum at 372 nm. Notably, the intensity of the characteristic negative band of the DNA at 260 nm increased significantly with increasing LDR values (Fig. 3B3).

Fluorescence-monitored quadruplex-DNA melting

The interactions of the ligands **1d** and **2a–c** with quadruplex DNA were investigated with representative quadruplex-forming oligonucleotide sequences. Firstly, the established FRET melting assay[17] was employed to assess the stabilization of the quadruplex structure upon association with the ligands. With this method, the propensity of a ligand to stabilize quadruplex-DNA towards unfolding was determined by monitoring the temperature-dependent emission of the dye-labeled quadruplex-forming oligonucleotide **F21T**, fluo-d($G_3TTA)_3G_3$-tamra (fluo: fluorescein; TAMRA: tetramethylrhodamine), because only in the quadruplex form a Förster resonance energy transfer (FRET) between the two dyes is possible. The quadruplex-forming oligonucleotide was chosen for first principal studies, as it is among the most commonly used substrates for this well-established assay.[17] The FRET melting experiments revealed that the ligand **2a** does not stabilize the G4-DNA **F21T**, even at high LDR = 5.0 (Table 1), while the ligands **1d**, **2b** and **2c** stabilize the G4-DNA **F21T** towards unfolding, as clearly indicated by the increase of the melting temperature, ΔT_m, of 27 °C (**1d**), 3 °C (**2b**) and 11 °C (**2c**) at LDR = 5.0 (Table 1). To assess whether this stabilization of G4-DNA is a general feature of the ligands **2b** and **2c** the same experiments were also performed with the representative quadruplex-forming oligonucleotides **FmycT** [fluo-d($TGAG_3TG_3TAG_3TG_3TA_2$)-tamra], **FkrasT** [fluo-d($AG_3CG_2TGTG_3A_2GAG_2A$)-tamra] and **Fa2T** [fluo-d($ACAG_4TGTG_4)_2$-tamra] (Table 1), all of which have been used already with this assay.[7,18] In all cases, the quadruplex structure is also stabilized to significantly more extent by ligand **2c** as compared with **2b**. Nevertheless, it was also observed that the degree of G4-DNA stabilization upon binding of ligand **2c** is not the same for the different oligonucleotides. Hence, the extent of stabilization decreases in the order **F21T** (ΔT_m = 11 °C), **FkrasT** (ΔT_m = 9.9 °C), **FmycT** (ΔT_m = 6.0 °C), and **Fa2T** (ΔT_m = 3.1 °C; all values at LDR = 5). To further assess the selectivity of the quadruplex stabilization by **2c**, the melting experiments were also performed in the presence of excess of the duplex-DNA forming oligonucleotide **ds26**.[17] Under these conditions, the ligand **2c** shows a thermal stabilization of the **F21T** by 7.5 °C at LDR = 5.0 (Table 1).

Table 1 Shift of melting temperature, ΔT_m, of the G4-DNA **F21T**, **FmycT**, **FkrasT** and **Fa2T** in the presence of the ligands **1d** and **2a–c**

	ΔT_m [a]/°C									
LDR	**1d** **F21T**	**2a**[b]	**2b**	**2c**	**2b** **Fa2T**	**2c**	**2b** **FmycT**	**2c**	**2b** **FkrasT**	**2c**
1.3	+9.3	−0.3	+0.7	+4.3 (2.9)	−0.2	<0.1	0.5	2.4	1.3	4.6
2.5	+21.6	+0.2	+1.6	+7.6 (5.0)	0.1	−0.2	−0.3	2.9	1.3	7.2
5.0	+27.1	−0.4	+3.3	+10.6 (7.5)	0.3	3.1	0.3	6.0	2.2	9.9

[a] c_{DNA} = 0.2 μM in Na-cacodylate buffer (pH = 7.2); estimated error: ±0.5 °C. Determined fluorimetrically based on the temperature-dependent change of FRET in **F21T**, **FmycT**, **FkrasT** and **Fa2T**. [b] With 1% v/v DMSO. ΔT_m values in parentheses determined in the presence of **ds26** d($CA_2TCG_2ATCGA_2T_2CGATC_2GAT_2G$) ($c$ = 3.0 μM).

Open Access Article. Published on 14 June 2019. Downloaded on 11/6/2025 9:33:02 PM.
This article is licensed under a Creative Commons Attribution-NonCommercial 3.0 Unported Licence.

Spectrometric titrations with quadruplex-DNA

The interactions of the ligands **1d**, **2b** and **2c** with the quadruplex-forming oligonucleotides **22AG** $dA(G_3TTA)_3G_3$ and **a2** $d(ACAG_4TGTG_4)_2$ were investigated by photometric and fluorimetric titrations (Fig. 4 and 5). Upon the addition of **22AG** or **a2**, the absorption maxima of **2b** (381 nm) and **2c** (366 nm) decreased with the development of red-shifted absorption maxima at 401 nm (**22AG**) and 406 nm (**a2**) for **2b** (Fig. 4A1 and B1), and 379 nm (**22AG**) and 382 nm (**a2**) for **2c** (Fig. 4A2 and B2). In both titrations of the ligand **2c** an isosbestic point was observed.

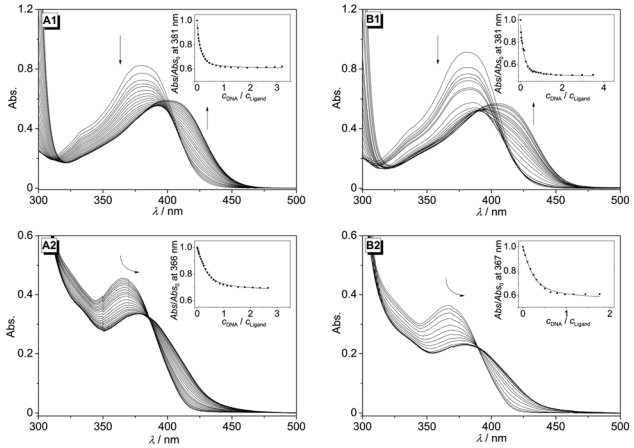

Fig. 4 Photometric titration of **2b** (1) and **2c** (2) (c = 20 μM) with **22AG** (A) and **a2** (B) (c_{DNA} = 200 μM) in K-phosphate buffer (pH = 7.0, 5% v/v DMSO), T = 20 °C. The arrows indicate the development of the absorption bands during the titration. Inset: Plot of absorption Abs./Abs.$_0$ *versus* c_{DNA}/c_{ligand}.

At the same time, the emission of derivatives **1d**, **2b** and **2c** is significantly quenched upon binding to **22AG** and **a2** (Fig. 5). The analysis of the resulting binding isotherms from the fluorimetric titrations of the ligands **1d**, **2b** and **2c** revealed binding constants of 1.5×10^6 M^{-1} (**1d**), 2.1×10^5 M^{-1} (**2b**) and 4.8×10^5 M^{-1} (**2c**) with **22AG** and 5.8×10^5 M^{-1} (**2b**) and 4.0×10^5 M^{-1} (**2c**) with **a2**.

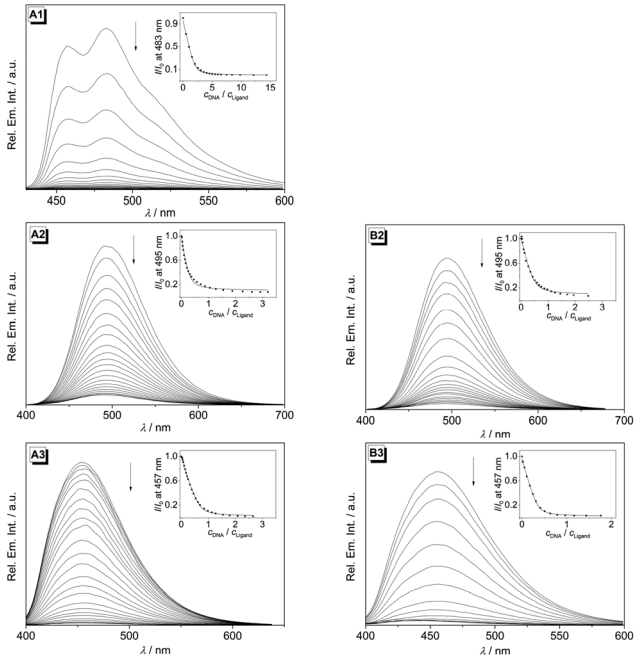

Fig. 5 Fluorimetric titration of **1d** (1), **2b** (2) and **2c** (3) (c = 20 μM) with **22AG** (A) and **a2** (B) (c_{DNA} = 200 μM) in K-phosphate buffer (pH = 7.0, 5% v/v DMSO), T = 20 °C; **1d**: λ_{ex} = 423 nm (**22AG**); **2b**: λ_{ex} = 390 nm (**22AG** and **a2**); **2c**: λ_{ex} = 385 nm (**22AG**) and 389 nm (**a2**). The arrows indicate the development of the emission bands during titration. Inset: Plot of relative emission intensity I/I_0 *versus* c_{DNA}/c_{ligand}.

^{1}H-NMR spectroscopic studies

Titrations of the diazoniastilbene **2c** to the quadruplex-forming oligonucleotide **Tel6** $d(T_2AG_3)$ was monitored by ^{1}H-NMR spectroscopy (Fig. 6). This hexanucleotide forms an equilibrium between monomeric and a terminally π-stacked dimeric G4-DNA $[d(T_2AG_3)]_4$ in aqueous solution[16,19] Although **Tel6** is only a very simplified quadruplex model as it does not contain the loop structures, such as *e.g.* **22AG**, this oligonucleotide or variations thereof are often employed for the NMR spectroscopic detection of terminally stacking G4-DNA ligands,[20] because the interpretation of the NMR data is straightforward. It should be noted that due to limited solubility at the employed concentration range only up to 1.5 molar equivalents of the ligand **2c** could be added. The titration of ligand **2c** to **Tel6** led to significant shifts of the ^{1}H NMR signals of the G4-DNA **Tel6** (Fig. 6). Thus, NMR signals of the guanine imino protons of the dimeric quadruplex broadened and shifted to high-field by 0.10–0.12 ppm on addition of up to 0.4 molar equivalents of **2c** and eventually disappeared during the course of titration. At the same time, the imino protons of the monomeric quadruplex were shifted by 0.27–0.32 ppm to higher field. Except for the proton signals of A3H2 and T1H6, most of the bands of the aromatic protons in the range of 6–8 ppm remained relatively sharp up to 0.8 molar equivalents of **2c** (*cf.* ESI, Fig. S2†). In addition, the

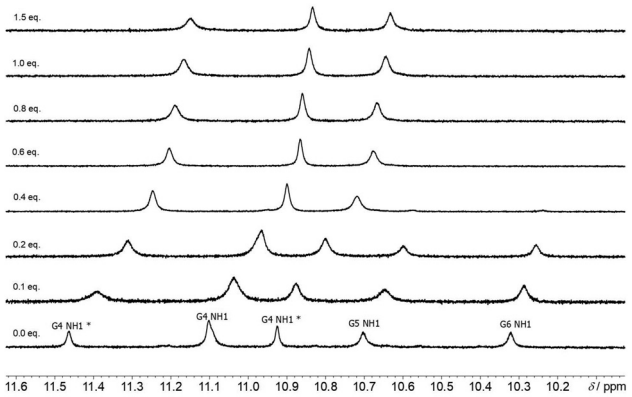

Fig. 6 The ^{1}H NMR spectra (600 MHz) of the imino protons of **Tel6** (2 mM in bases) in K-phosphate buffer ($H_2O : D_2O$ = 9 : 1; 95 mM, pH 7.0; T = 25 °C) with increasing amount of **2c**; * = monomeric quadruplex.

Open Access Article. Published on 14 June 2019. Downloaded on 11/6/2025 9:33:02 PM.
This article is licensed under a Creative Commons Attribution-NonCommercial 3.0 Unported Licence.

^{1}H-NMR signals of ligand **2c** also developed and shifted during the titration. As a general trend, the signals of the protons H2, H4, H6, and H7 were shifted to lower field by up to 0.4 ppm upon association of the ligand with the DNA, whereas the proton H8 is slightly shifted to higher field and H5 does not experience a significant shift (*cf.* ESI, Fig. S2†).

Discussion

The results from the spectrometric DNA titrations with ct DNA clearly indicate the binding interactions between duplex DNA and the aza- and azoniastilbene derivatives **2a–c**; however, with significantly different affinity and binding mode. Thus, the association of the charge neutral derivative **2a** with ct DNA is rather weak, as shown by the lack of a shift of absorption band during the photometric DNA titration and by the inefficient fluorescence quenching by DNA. Moreover, the positive LD signal of the DNA-bound ligand indicates groove binding. As the development and band structure of the ICD bands does not reveal a clear trend and depends strongly on the ligand concentration, it is assumed that this ligand forms only loosely bound aggregates along the DNA grooves whose actual structure depends on the ligand–DNA ratio. This assumption is supported by the observation that the development of absorption bands of **2a** during titration is not characteristic of a DNA binder, but rather indicates the random association of the hardly soluble compound along the DNA backbone, as shown by the plain decrease of absorption band with no significant shift. Therefore the determined binding constant is rather an aggregation constant of the ligand. This undirectional binding mode of this ligand to DNA is explained by the lack of a positive charge, which is usually required for high affinity of DNA ligands. In contrast, the ligands **2b** and **2c** exhibit the characteristic spectroscopic features of DNA intercalators, specifically polycyclic azoniahetarenes,[10c,21] upon complex formation[22] namely a hypochromic effect and red shift of the absorption band, fluorescence quenching, the development of a weak positive or negative ICD band, typical binding constants (**2b**: 5.1×10^4 M^{-1}, **2c**: 2.0×10^5 M^{-1}) and – mostly indicative of the binding mode – a negative LD band in the ligand absorption range. It is tempting to conclude that the ligands **2b** and **2c** have different alignments in the intercalation site as the ICD signals develop with different phase. However, the sign of the ICD signals depends on the relative orientation of the transition dipole moments of the ligand and the DNA base pairs. Considering dipole moments of the ligands that are aligned along the long molecular axis in **2b** and along the short molecular axis in **2c**, as deduced from the substitution pattern, both ligands intercalate into DNA with the long molecule axis perpendicular to the long axis of the binding site.

In addition, it was demonstrated that the ligands **2b** and **2c** bind to quadruplex DNA also, as shown exemplarily with the two representative DNA forms **22AG** and **a2** as well as with the dye labeled quadruplex-forming oligonucleotides **F21T**, **FmycT**, **FkrasT** and **Fa2T**. With regard to the association with quadruplex DNA, the azo- and azoniastilbene derivatives **2a–c** show a similar trend of binding constants as with duplex DNA. It should be noted that the binding constants of the ligands with ct DNA and quadruplex DNA appear to be the same (*e.g.* for **2c**: $K_B^{ctDNA} = 2.0 \times 10^5$ M^{-1} $K_B^{22AG} = 4.8 \times 10^5$ M^{-1}), however; they were determined in solutions with different ionic strength (10 mM BPE buffer *versus* 95 mM K-phosphate buffer). Therefore, they cannot be directly compared because it is known that the binding constants, especially the ones of cationic ligands, decrease with increasing ionic strength. In fact, a control experiment showed that **2c** has a significantly smaller binding constant with ct DNA of $K_B = 6.7 \times 10^4$ M^{-1} at higher ionic strength (*cf.* ESI†). In general, with the increasing number of positive charges in the molecule the binding interaction with the DNA is getting stronger; however, this effect is more pronounced in the case of quadruplex DNA **22AG**. Thus, the uncharged derivative **2a** does not have a stabilizing effect on quadruplex DNA which indicates a very weak binding interaction. In contrast, the positively charged stilbene derivatives **2b** and **2c** induce a significant stabilization of the quadruplex DNA **F21T**, **FmycT**, **FkrasT** and **Fa2T** toward unfolding, and this effect is much stronger in the case of the dicationic derivative **2c** than with the monocationic one. This difference may be explained by the effect of the positive charge, namely attractive Coulomb interactions with the phosphate backbone as well as thermodynamically favorable release of counter ions from the grooves and their subsequent solvation in the aqueous medium.[9] The ligands **2b** and **2c** also bind to the ILPR DNA **a2** as indicated by the spectrometric titrations and binding constants that are in the same range as the ones observed with **22AG**. However, the stabilization of the ILPR quadruplex toward unfolding is not very pronounced according to the relatively low shifts of melting temperature of **Fa2T** upon ligand binding. This difference between binding constants and ΔT_m values may be explained by the different buffer solutions that are used in each experiment.[18] Moreover, even the rather moderate increase of the DNA melting temperature of **Fa2T** is indicative of ligand binding, because similar results were obtained with the well-established quadruplex ligands thiazole orange (ΔT_m = 3.1 °C), porphyrine **TMPyP4** (ΔT_m = 6.3 °C) and coralyne (ΔT_m = 1.8 °C) under identical conditions.[18]

In the case of ligand **2c**, the association with the quadruplex-forming oligonucleotide **Tel6** as simple model was further confirmed by NMR-spectroscopic analysis. The broadening and significant upfield-shift of the imino protons of the guanine residues of the quadruplex usually indicate a terminal π-stacking of the ligand. Although it may be tempting to assume intercalation, this mode of binding is usually not favorable in quadruplex structures.[23] Moreover, the significant shifts of the ligand protons during complex formation may be explained by the π-stacking to a terminal quartet and the positioning of the ligand protons in the anisotropic cones of the guanine quartet.

Open Access Article. Published on 14 June 2019. Downloaded on 11/6/2025 9:33:02 PM.
This article is licensed under a Creative Commons Attribution-NonCommercial 3.0 Unported Licence.

The initial goal of this study was the comparison of the DNA-binding properties of the stilbene derivatives **2a–c** with the ones of the structurally resembling, quadruplex-binding dibenzochrysenes **1a–c**. Specifically, it should be tested whether the increased structural flexibility of the stilbenes – while maintaining a similar longitudinal extension of the π-system – increases the affinity of the former ligands to DNA. Indeed, it was observed that the structurally flexible diazoniastilbene **2c** has a stabilizing effect on quadruplex DNA **F21T** (ΔT_m = 11 °C; LDR = 5.0); but the diazoniabenzochrysene derivatives **1a–c** have been shown to induce an even larger increase of the melting temperature of quadruplex DNA **F21T** under almost identical conditions (ΔT_m = 6–19 °C, LDR = 5.0).[10b] In the case of **1a**[10b] and **2c** (Table 1), the thermal stabilization of the quadruplex is only marginally influenced by the presence of duplex DNA **ds26**, indicating a high selectivity of these ligands for quadruplex DNA relative to duplex. Nevertheless, this selectivity appears to be slightly more pronounced for the rigid diazoniadibenzochrysene **1a** because the decrease of the melting temperature is smaller ($\Delta\Delta T_m$ = −2.5 °C, LDR = 5.0) than the one observed with **2c** ($\Delta\Delta T_m$ = −3.1 °C). Moreover, the binding constant of **2c** with quadruplex DNA **22AG** is about half as large as the ones of the ligands **1a–c** (**2c**: 4.8×10^5 M^{-1} *versus* **1a–c**: $2.5–3 \times 10^6$ M^{-1} [10b]). These observations imply that the gain in flexibility in ligand **2c** as compared with the structurally rigid dibenzochrysenes **1a–c** does not compensate the loss of overall π-surface. Thus, these results show in a direct comparison of two ligands with resembling extent and shape of the π system that at least under equilibrium conditions the π-stacking or dispersion interactions of a ligand contribute more to the affinity of a ligand to terminal binding sites of the quadruplex structure than its flexibility, although the latter would allow the ligand to adjust its conformation within the binding site in an induced-fit process. Although it may be obvious from literature data[1,7] that both rigid and flexible ligands can bind to quadruplex DNA with reasonable affinity and selectivity, to the best of our knowledge there is only one direct and explicit comparison reported between two types of ligands with closely resembling ligand structures that mainly differ in terms of rigidity of the π system.[12] However, it should be emphasized that the latter study is not directly comparable with the results presented herein, because even the "rigid" ligands contain flexible substituents that may influence the overall binding affinity to G4-DNA. Complementary to those findings, our results could be helpful for ligand design, because we present the counterintuitive observation that the affinity and selectivity of a given flexible ligand may be even increased by the introduction of more rigidity. This small but significant effect may be explained by thermodynamic factors, because the rigid ligand does not loose conformational freedom, thus causing no additional entropic penalty, upon transfer from the solution to the constrained binding site.

Notably, the differences of the ligand-induced shifts of quadruplex melting temperatures on addition of **2b** and **2c** ($\Delta\Delta T_m$ = 7 °C (**F21T**) and $\Delta\Delta T_m$ = 3 °C (**Fa2T**) at LDR = 5) appear to be too large to be solely caused by the different charges and may need further attention. Considering the known, but still rather unexplored "methyl effect" of DNA ligands, the increased affinity of **2c** may also be caused by its methyl substituents, *i.e.* supported by additional dispersion interactions between the methyl groups and the hydrophobic binding site.[24] To assess whether this methyl effect also affects the quadruplex-stabilizing properties of the diazoniadibenzo [*b*,*k*]chrysene scaffold and to have a better comparison with **2c**, the dimethyl-substituted derivative **1d** was also investigated in this study as it resembles the methyl-substitution pattern of **2c**. Moreover, it was assumed that due to its close structural resemblance with the parent compounds **1a–c** the derivative **1d** also binds to quadruplex DNA through terminal π stacking. In fact, the methyl-substituted derivative **1d** also induces a much better stabilization of the quadruplex DNA **F21T** toward thermal unfolding as the parent compounds **1a–c** (ΔT_m = 27 °C; LDR = 5.0), although with slightly smaller binding constant. Unfortunately, the bad solubility of some **1d**-DNA complexes hampered its complete investigation. But at least the obtained results are in agreement with the ones with ligand **2c**, which indicates that a methyl effect may operate in quadruplex ligands, presumably based on attractive dispersion interactions of the methyl substituents with the hydrophobic binding site. Nevertheless, this assumption has to be verified in a systematic study with a larger series of methyl-substituted ligand derivatives.

Conclusions

We have shown that aza- and azoniastilbene derivatives **2a–c**, *i.e.* compounds with almost the same spatial dimensions and steric demand, bind to DNA with an affinity and selectivity that depends significantly on the number of positive charges. Whereas the charge neutral derivative **2a** only binds non-specifically to the DNA backbone of duplex DNA, the ionic compounds **2b** and **2c** are typical DNA intercalators. Most notably, the bis-quinolinium derivative **2c** binds to quadruplex DNA with moderate affinity and also induces a pronounced stabilization of the quadruplex DNA towards thermal denaturation, presumably caused by an additional methyl effect. In contrast to the proposed properties of the stilbene derivatives **2b** and **2c**, these ligands have a significantly weaker stabilizing effect on quadruplex DNA than the dibenzochrysene derivatives **1a–d**. From this observation we carefully conclude that the increased flexibility of a quadruplex-DNA ligand does not lead to stronger interactions with the quadruplex DNA as compared with rigid ligands that have essentially the same size and extent of π-system. Certainly, this finding has to be further substantiated with a larger series of ligands and quadruplex forms; however, the present study already reveals that structural rigidity and lack of conformational freedom, as in the diazoniadibenzochrysene series, is not a disadvantage with respect to quadruplex-DNA binding.

 This journal is © The Royal Society of Chemistry 2019

Open Access Article. Published on 14 June 2019. Downloaded on 11/6/2025 9:33:02 PM.
This article is licensed under a Creative Commons Attribution-NonCommercial 3.0 Unported Licence.

Experimental

Equipment

Melting points were determined with a BÜCHI 545 (Büchi, Flawil, CH) and are uncorrected. NMR spectra were recorded on a Bruker AV 400 (^{1}H: 400 MHz and ^{13}C: 100 MHz) or on a Varian VNMR-S 600 (^{1}H: 600 MHz, ^{13}C: 150 MHz) at 20 °C; chemical shifts are given in ppm (δ) values relative to tetramethylsilane (TMS) as internal standard (δ = 0.0). Combustion analyses were carried out by Mr Rochus Breuer (Organic Chemistry I, University of Siegen). Mass spectra were recorded on a Finnigan LCQ deca (driving voltage: 6 kV, impingement gas: argon, capillary temperature: 200 °C, auxiliary gas: nitrogen). Photometric titrations were recorded with a Varian Cary 100 Bio. A Varian Cary Eclipse spectrometer was used for the spectrofluorimetric analyses. The CD and *flow*-LD measurements were performed on a Chirascan spectrometer (Applied Photophysics).

Materials

Commercially purchased reagents were used without further purification. Chemicals were obtained from Alfa Aesar GmbH & Co. KG, Karlsruhe, Germany (*N*-bromosuccinimide, 3-bromoquinoline, ethenyltriethylsilane), Acros Organics [*n*-butyllithium solution (2.5 M in hexane), 2-butenoic acid, 4-pyridinecarbonitrile]. 1,5-di(bromomethyl)naphthalene (**5**)[11] 2-(2-methyl-(1,3)-dioxolan-2-yl)pyridine (**6**),[13] 2-methylquinolizinium bromide (**3**)[25] and (*E*)-1,2-di(quinolin-3-yl)ethane (**2a**)[15] were prepared according to literature protocols. The oligonucleotides fluo-d($G_3T_2AG_3T_2AG_3T_2AG_3$)–tamra (**F21T**, fluo = fluoresceine; tamra = tetramethylrhodamine), **FmycT** [fluo-d($TGAG_3TG_3TAG_3TG_3TA_2$)-tamra], **FkrasT** [fluo-d($AG_3CG_2TGTG_3A_2GAG_2A$)-tamra], **Fa2T** fluo-d($ACAG_4TGTG_4$)$_2$-tamra, d($AG_3T_2AG_3T_2AG_3T_2AG_3$) (**22AG**), **a2** d($ACAG_4TGTG_4$)$_2$ and d(T_2AG_3) (**Tel6**) were purchased from Metabion or Biomers and ct DNA was purchased from Merck and used without any further purification. DNA solutions in buffer were prepared according to published procedures;[26] BPE buffer (pH 7.0): 6.0 mM Na_2HPO_4, 2.0 mM NaH_2PO_4, 1.0 mM Na_2EDTA; Na-cacodylate buffer (pH 7.2–7.3): 10 mM $Na(CH_3)_2AsO_2 \cdot 3H_2O$, 10 mM KCl, 90 mM LiCl; K-phosphate buffer (pH 7.0): 25 mM K_2HPO_4, 70 mM KCl.

Methods

The spectrophotometric, spectrofluorimetric and CD-spectroscopic titrations with DNA, and the thermal DNA denaturation studies were performed according to reported protocols (*cf.* ESI†).[10a,b] To ensure a sufficient solubility of the ligands during the titrations, all experiments were performed with 5% v/v DMSO as cosolvent. Binding constants of ligand–DNA complexes were determined by fitting of the experimental data from the photometric and fluorimetric DNA titrations to the theoretical model according to the published procedure (*cf.* ESI†).[10a,27]

Synthesis of 1,5-bis{[1-(2-methyl-1,3-dioxolan-2 yl)pyridinium]methyl}naphtalenebis(tetrafluoroborate) (7). A solution of 1,5-di(bromomethyl)naphthalene (**5**)[11] (0.75 g, 2.39 mmol) and 2-(2-methyl-(1,3)-dioxolan-2-yl)pyridine (**6**)[13] (1.09 g, 6.60 mmol) in DMSO (15 mL) were stirred at r.t. for 10 d. The yellow brown solution was added into EtOAc (100 mL). The precipitated crude solid was filtered and washed with EtOAc and Et_2O. The solid was recrystalized from MeOH (0.5 mL, with added HBF_4) to obtain product **7** (600 mg, 0.92 mmol, 36%); mp = 252–254 °C (dec.). – ^{1}H NMR (400 MHz, DMSO-d_6): δ = 1.84 (6 H, s, CH_3), 3.73–3.76 (4 H, m, CH_2), 4.02–4.08 (4 H, m, CH_2), 6.25 (4 H, s, CH_2N^+), 7.43 (1 H, d, ^3J = 7 Hz, CH), 7.63 (2 H, dd, ^3J = 8 Hz, CH), 7.99 (2 H, d, ^3J = 9 Hz, CH), 8.20 (2 H, ddd, ^3J = 8 Hz, ^3J = 6 Hz, ^4J = 1 Hz, CH), 8.39 (2 H, d, ^3J = 8 Hz, CH), 8.74 (2 H, dd, ^3J = 9 Hz, ^3J = 8 Hz, CH), 9.05 (2 H, d, ^3J = 6 Hz, CH). – ^{13}C-NMR (DMSO-d_6, 100 MHz): 26.0, 61.1, 65.3, 106.1, 109.1, 125.5, 125.7, 126.9, 128.3, 128.9, 132.2, 133.9, 147.6, 148.8, 156.3. – El. anal. for $C_{30}H_{32}N_2B_2F_8O_4 \times H_2O$ (676.21) calcd (%): C 53.29, H 5.07, N 4.14, found: C 52.93; H 4.13; N 4.21.

Synthesis of 4a,12a-diazonia-8,16-dimethyldibenzo[*b*,*k*]chrysenebis(tetrafluoroborate) (1d). The bispyridinium **7** (295 mg, 0.45 mmol) was stirred in PPA (3.06 g) at 150 °C for 24 h. The mixture was cooled to 100 °C and saturated aqueous solution of $NaBF_4$ (10 mL) was added. After cooling slowly to r.t. the aquesous solution was extracted with $MeNO_2$. The organic layer was separated, dried with Na_2SO_4, and the solvent was evaporated to obtain the product **1d** as yellow needles (179 mg, 0.34 mmol, 75%); mp >300 °C. – ^{1}H NMR (400 MHz, DMF-d_7): δ = 3.49 (6 H, s, CH_3), 8.34 (2 H, dd, ^3J = 7 Hz, CH), 8.49 (2 H, dd, ^3J = 8 Hz, CH), 9.14 (2 H, d, ^3J = 9 Hz, CH), 9.17 (2 H, d, ^3J = 9.4 Hz, CH), 9.69 (2 H, d, ^3J = 9 Hz, CH), 9.77 (2 H, d, ^3J = 7 Hz, CH), 11.62 (2 H, s, CH). – ^{13}C-NMR (DMF-d_7, 100 MHz): δ = 13.4 (CH_3), 122.8 (Cq), 123.0 (CH), 124.1 (CH), 125.5 (CH), 128.2 (CH), 128.8 (Cq), 132.4 (Cq), 132.9 (CH), 133.9 (Cq), 135.8 (CH). – El. anal. for $C_{26}H_{20}N_2B_2F_8 \cdot 2\ H_2O$ (563.33) calcd (%): C 54.78, H 4.24, N 4.91; found C 55.37, H 4.01, N 5.44.

Synthesis of (*E*)-2-(2-(naphthalene-2-yl)vinyl)quinolizinium bromide (2b). A solution of 2-methylquinolizinium bromide (**3**)[25] (448 mg, 2.00 mmol), 2-naphthaldehyde (**4**) (469 mg, 3.00 mmol) and piperidine (0.20 mL) in MeOH (5 mL) was stirred under reflux for 5 h. The reaction mixture was cooled to r.t. and filtered. The filter cake was washed with cold MeOH and then with Et_2O. The obtained orange-colored solid was recrystalized from MeOH to give the product **2b** (450 mg, 1.24 mmol, 62%) as orange crystals (note: due to its photoreactivity this compound should be handled in the dark); mp = 272–274 °C (dec.). ^{1}H NMR (600 MHz, DMSO-d_6): δ = 7.55–7.60 (2 H, m, 1′-H, 2′-H), 7.70 (1 H, d, ^3J = 16 Hz, 4′-H), 7.92–8.04 (5 H, m, 3-H, 9-H, 7′-H, 8′-H, 9′-H), 8.12 (1 H, d, ^3J = 16 Hz, 5′-H), 8.19 (1 H, s, 10′-H), 8.31 (1 H, t, ^3J = 8 Hz, 8-H), 8.43–8.50 (2 H, m, 7-H, 6′-H), 8.60 (1 H, s, 1-H), 9.26 (1 H, d, ^3J = 8 Hz, 4-H), 9.33 (1 H, d, ^3J = 7 Hz, 6-H). – ^{13}C NMR (150 MHz, DMSO-d_6): δ = 120.3, 122.8, 123.0, 123.6, 124.3, 126.9, 126.9, 127.3, 127.7, 128.4, 128.7, 129.1, 133.0, 133.1, 133.5, 136.6, 136.9, 138.4, 142.8, 144.9. – MS (ESI+): *m*/*z* (rel. intensity) = 282 (100) [M^+]. – El. anal. for $C_{21}H_{16}BrN \times H_2O$ (368.28) calcd (%): C 66.33, H 4.77, N 3.68, found: C 66.41; H 4.71; N 3.64.

Open Access Article. Published on 14 June 2019. Downloaded on 11/6/2025 9:33:02 PM.
This article is licensed under a Creative Commons Attribution-NonCommercial 3.0 Unported Licence.

Synthesis of (*E*)-3,3′-(ethane-1,2-diyl)bis(1-methylquinolin-1-ium) (2c). In a 200 mL sealed tube, a mixture of **2a**[15] (141 mg, 0.50 mmol) in MeI (5.0 mL) was stirred at 140 °C for 5 h. The reaction mixture was cooled to r.t. and Et_2O (30 mL) was added. The yellow precipitate was filtered and washed with Et_2O. The remaining solid was dissolved in a small amount of MeOH (100 ml) and the solid was passed through a bromide-saturated ion-exchange column (DOWEX®1 × 8) three times. The solvent was evaporated and the solid was re-crystalized from MeOH/MeCN to obtain product **2c** as a yellow solid (note: due to its photoreactivity this compound was handled in the dark); mp = 292–294 °C. ^{1}H NMR (600 MHz, DMSO-d_6): δ = 4.71 (6 H, s, 2 × CH_3), 7.94 (2 H, s, 1′-H, 2′-H), 8.11 (2 H, t, ^3J = 8 Hz, 6-H, 6″-H), 8.28–8.32 (2 H, m, 7-H, 7″-H), 8.53 (2 H, d, ^3J = 8 Hz, 5-H, 5″-H), 8.55 (2 H, d, ^3J = 9 Hz, 8-H, 8″-H), 9.40 (2 H, s, 4-H, 4″-H), 9.92 (2 H, s, 2-H, 2″-H). – ^{13}C NMR (150 MHz, DMSO-d_6): δ = 45.8, 119.3, 127.8, 129.1, 129.9, 130.5, 130.6, 135.5, 137.5, 142.9, 149.2. – El. anal. for $C_{22}H_{20}Br_2{\cdot}0.5\ H_2O$ (508.25) calcd (%): C 51.99, H 4.76, N 5.51, found: C 52.28; H 4.78; N 5.55.

Conflicts of interest

There are no conflicts to declare.

Acknowledgements

Generous support by the Deutsche Forschungsgemeinschaft is gratefully acknowledged. We thank Ms Jennifer Hermann, Ms Sandra Uebach and Dr Stefanie Müller for technical assistance.

Notes and references

1 (*a*) C. K. Kwok and C. J. Merrick, *Trends Biotechnol.*, 2017, **35**, 997; (*b*) S. Neidle, *Nat. Rev. Chem.*, 2017, **1**, 0041; (*c*) S. Neidle, *J. Med. Chem.*, 2016, **59**, 5987; (*d*) D. Rhodes and H. J. Lipps, *Nucleic Acids Res.*, 2015, **43**, 8627; (*e*) S. Balasubramanian, L. H. Hurley and S. Neidle, *Nat. Rev. Drug Discovery*, 2011, **10**, 261; (*f*) G. W. Collie and G. N. Parkinson, *Chem. Soc. Rev.*, 2011, **40**, 5867.

2 (*a*) T. Caneque, S. Müller and R. Rodriguez, *Nat. Rev. Chem.*, 2018, **2**, 202; (*b*) A. Laguerre, J. M. Y. Wong and D. Monchaud, *Sci. Rep.*, 2016, **6**, 32141; (*c*) V. S. Chambers, G. Marsico, J. M. Boutell, M. Di Antonio, G. P. Smith and S. Balasubramanian, *Nat. Biotechnol.*, 2015, **33**, 877.

3 (*a*) J. L. Huppert and S. Balasubramanian, *Nucleic Acids Res.*, 2007, **35**, 406; (*b*) J. L. Huppert, A. Bugaut, S. Kumari and S. Balasubramanian, *Nucleic Acids Res.*, 2008, **36**, 6260; (*c*) A. Verma, V. K. Yadav, R. Basundra, A. Kumar and S. Chowdhury, *Nucleic Acids Res.*, 2009, **37**, 4194.

4 (*a*) C. L. Grand, T. J. Powell, R. B. Nagle, D. J. Bearss, D. Tye, M. Gleason-Guzman and L. H. Hurley, *Proc. Natl. Acad. Sci. U. S. A.*, 2004, **101**, 6140; (*b*) A. Siddiqui-Jain, C. L. Grand, D. J. Bearss and L. H. Hurley, *Proc. Natl. Acad. Sci. U. S. A.*, 2002, **99**, 11593; (*c*) S. Balasubramanian, L. H. Hurley and S. Neidle, *Nat. Rev. Drug Discovery*, 2011, **10**, 261; (*d*) Y. Li, J. Syed, Y. Suzuki, S. Asamitsu, N. Shioda, T. Wada and H. Sugiyama, *ChemBioChem*, 2016, **17**, 928; (*e*) G. W. Collie and G. N. Parkinson, *Chem. Soc. Rev.*, 2011, **40**, 5867; (*f*) S. J. Adam, C. L. Grand, D. J. Bearss and L. H. Hurley, *Proc. Natl. Acad. Sci. U. S. A.*, 2002, **99**, 11593; (*g*) S. Kumari, A. Bugaut, J. L. Huppert and S. Balasubramanian, *Nat. Chem. Biol.*, 2007, **3**, 218.

5 (*a*) S. Balasubramanian and S. Neidle, *Curr. Opin. Chem. Biol.*, 2009, **13**, 345; (*b*) R. Hänsel-Hertsch, M. Di Antonio and S. Balasubramanian, *Nat. Rev. Mol. Cell Biol.*, 2017, **18**, 279.

6 (*a*) R. C. Monsen and J. O. Trent, *Biochimie*, 2018, **152**, 134; (*b*) H.-S. Lee, M. Carmena, M. Liskovykh, E. Peat, J.-H. Kim, M. Oshimura, H. Masumoto, M.-P. Teulade-Fichou, Y. Pommier, W. C. Earnshaw, V. Larionov and N. Kouprina, *Cancer Res.*, 2018, **78**, 6282.

7 (*a*) S. Asamitsu, T. Bando and H. Sugiyama, *Chem. – Eur. J.*, 2019, **25**, 417; (*b*) E. Ruggiero and S. N. Richter, *Nucleic Acids Res.*, 2018, **46**, 3270; (*c*) T. Che, Y.-Q. Wang, Z.-L. Huang, J.-H. Tan, Z.-S. Huang and S.-B. Chen, *Molecules*, 2018, **23**, 493; (*d*) Y. Xu, *Chem. Soc. Rev.*, 2011, **40**, 2719; (*e*) A. Ali and S. Bhattacharya, *Bioorg. Med. Chem. Lett.*, 2014, **22**, 4506; (*f*) P. Murat, Y. Singh and E. Defrancq, *Chem. Soc. Rev.*, 2011, **40**, 5293.

8 (*a*) S. Bhaduri, N. Ranjan and D. P. Arya, *Beilstein J. Org. Chem.*, 2018, **14**, 1051; (*b*) A. Rescifina, C. Zagni, M. G. Varrica, V. Pistarà and A. Corsaro, *Eur. J. Med. Chem.*, 2014, **74**, 95.

9 H. Ihmels and L. Thomas, in *Materials Science of DNA Chemistry*, ed. J.-I. Jin, CRC Press, Boca Raton, 2011, p. 49.

10 (*a*) A. Granzhan, H. Ihmels and K. Jäger, *Chem. Commun.*, 2009, 1249; (*b*) K. Jäger, J. W. Bats, H. Ihmels, A. Granzhan, S. Uebach and B. O. Patrick, *Chem. – Eur. J.*, 2012, **18**, 10903; (*c*) A. Granzhan and H. Ihmels, *Synlett*, 2016, 1775; (*d*) H. Ihmels, K. Löhl, T. Paululat and S. Uebach, *New J. Chem.*, 2018, **42**, 13813.

11 A. de Cian, E. DeLemos, J.-L. Mergny, M.-P. Teulade-Fichou and D. Monchaud, *J. Am. Chem. Soc.*, 2007, **129**, 1856.

12 B. Prasad, J. Jamroskovic, S. Bhowmik, R. Kumar, T. Romell, N. Sabouri and E. Chorell, *Chem. – Eur. J.*, 2018, **24**, 7926.

13 W. Sbliwa, G. Matusiak and B. Bachowska, *Croat. Chem. Acta*, 2006, **79**, 513.

14 (*a*) M.-Q. Wang, Y. Wu, Z.-Y. Wang, Q.-Y. Chen, F.-Y. Xiao, Y.-C. Jiang and A. Sang, *Dyes Pigm.*, 2017, **145**, 1; (*b*) M.-Q. Wang, J. Xu, L. Zhang, Y. Liao, H. Wei, Y.-Y. Yin, Q. Liu, M.-Q. Wang, W.-X. Zhu, Z.-Z. Song, S. Li and Y.-Z. Zhang, *Bioorg. Med. Chem. Lett.*, 2015, **25**, 5672; (*c*) R. Chennoufi, H. Bougherara, N. Gagey-Eilstein, B. Dumat, E. Henry, F. Subra, S. Bury-Moné, F. Mahuteau-Betzer, P. Tauc, M.-P. Teulade-Fichou and E. Deprez, *Sci. Rep.*, 2016, **6**, 21458; (*d*) M.-Q. Wang, J. Xu, L. Zhang,

 This journal is © The Royal Society of Chemistry 2019

Open Access Article. Published on 14 June 2019. Downloaded on 11/6/2025 9:33:02 PM.
This article is licensed under a Creative Commons Attribution-NonCommercial 3.0 Unported Licence.

Y. Liao, H. Wei, Y.-Y. Yin, Q. Liu and Y. Zhang, *Bioorg. Med. Chem.*, 2019, **27**, 552.

15 X. Zhang, E. L. Clennan, N. Arulsamy, R. Weber and J. Weber, *J. Org. Chem.*, 2016, **81**, 5474.

16 Y. Wang and D. J. Patel, *Biochemistry*, 1992, **31**, 8112.

17 (*a*) D. Renčiuk, J. Zhou, L. Beautepaire, A. Guédin, A. Bourdoncle and J.-L. Mergny, *Methods*, 2012, **57**, 122; (*b*) A. de Cian, L. Guittat, M. Kaiser, B. Saccà, S. Amrane, A. Bourdoncle, P. Alberti, M.-P. Teulade-Fichou, L. Lacroix and J.-L. Mergny, *Methods*, 2007, **42**, 183.

18 (*a*) D. Dzubiel, H. Ihmels, M. M. A. Mahmoud and L. Thomas, *Beilstein J. Org. Chem.*, 2014, **10**, 2963; (*b*) J. W. Yan, S.-B. Chen, H.-Y. Liu, W.-J. Ye, T.-M. Ou, J.-H. Tan, D. Li, L.-Q. Gu and Z.-S. Huang, *Chem. Commun.*, 2014, **50**, 6927; (*c*) S. Paramasivan and P. H. Bolton, *Nucleic Acids Res.*, 2008, **36**, e106; (*d*) J. Carvalho, T. Quintela, N. M. Gueddouda, A. Bourdoncle, J. Mergny, G. F. Salgado, J. A. Queiroz and C. Cruz, *Org. Biomol. Chem.*, 2018, **16**, 2776; (*e*) A. Chauhan, S. Paladhi, M. Debnath and J. Dash, *Org. Biomol. Chem.*, 2016, **14**, 5761; (*f*) J. Lavrado, P. M. Borralho, S. A. Ohnmacht, R. E. Castro, C. M. P. Rodrigues, R. Moreira, D. J. V. A. dos Santos, S. Neidle and A. Paulo, *ChemMedChem*, 2013, **8**, 1648.

19 G. A. Michelotti, E. F. Michelotti, A. Pullner, R. C. Duncan, D. Eick and D. Levens, *Mol. Cell. Biol.*, 1996, **16**, 2656.

20 See *e.g.* (*a*) P. Kumar and R. Barthwal, *Biochimie*, 2018, **147**, 153; (*b*) K. Padmapriya and R. Barthwal, *Biochim. Biophys. Acta*, 2017, **1861**, 37; (*c*) L. Scaglioni, R. Mondelli, R. Artali, F. R. Sirtori and S. Mazzini, *Biochim. Biophys. Acta, Gen. Subj.*, 2016, **1860**, 1129; (*d*) K. Padmapriya and R. Barthwal, *Bioorg. Med. Chem. Lett.*, 2016, **26**, 4915; (*e*) S. Tripathi, T. P. Pradeep and R. Barthwal, *ChemBioChem*, 2016, **17**, 554; (*f*) T. P. Pradeep and R. Barthwal, *Biochimie*, 2016, **128**, 59; (*g*) W. Gai, Q. Yang, J. Xiang, W. Jiang, Q. Li, H. Sun, A. Guan, Q. Shang, H. Zhang and Y. Tang, *Nucleic Acids Res.*, 2013, **41**, 2709; (*h*) R. Ferreira, R. Artali, J. Farrera-Sinfreu, F. Albericio, M. Royo, R. Eritja and S. Mazzini, *Biochim. Biophys. Acta, Gen. Subj.*, 2011, **1810**, 769; (*i*) E. Gavathiotis, R. A. Heald, M. F. G. Stevens and M. S. Searle, *Angew. Chem., Int. Ed.*, 2001, **40**, 4749.

21 (*a*) S. K. Manna, A. Mandal, S. K. Mondal, A. K. Adak, A. Jana, S. Das, S. Chattopadhyay, S. Roy, S. K. Ghorai, S. Samanta, M. Hossain and M. Baidya, *Org. Biomol. Chem.*, 2015, **13**, 8037; (*b*) B. Abarca, R. Custodio, A. M. Cuadro, D. Sucunza, A. Domingo, F. Mendicuti, J. Alvarez-Builla and J. J. Vaquero, *Org. Lett.*, 2014, **16**, 3464; (*c*) R. M. Suárez, P. Bosch, D. Sucunza, A. M. Cuadro, A. Domingo, F. Mendicuti and J. J. Vaquero, *Org. Biomol. Chem.*, 2015, **13**, 527; (*d*) P. Bosch, D. Sucunza, F. Mendicuti, A. Domingo and J. J. Vaquero, *Org. Chem. Front.*, 2018, **5**, 1916.

22 M. M. Aleksic and V. Kapetanovic, *Acta Chim. Slov.*, 2014, **61**, 555.

23 (*a*) E. Gavathiotis, R. A. Heald, M. F. G. Stevens and M. S. Searle, *Angew. Chem., Int. Ed.*, 2001, **40**, 4749; (*b*) H. Mita, T. Ohyama, Y. Tanaka and Y. Yamamoto, *Biochemistry*, 2006, **45**, 6765; (*c*) d. S. M. Webba, *Methods*, 2007, **43**, 264.

24 (*a*) A. K. F. Martensson and P. Lincoln, *Phys. Chem. Chem. Phys.*, 2018, **20**, 11336; (*b*) E. J. Barreiro, A. E. Kümmerle and C. A. M. Fraga, *Chem. Rev.*, 2011, **111**, 5215; (*c*) C. S. Leung, S. S. F. Leung, J. Tirado-Rives and W. L. Jorgensen, *J. Med. Chem.*, 2012, **55**, 4489; (*d*) B. Rajendar, Y. Sato, S. Nishizawa and N. Teramae, *Bioorg. Med. Chem. Lett.*, 2007, **17**, 3682; (*e*) B. Rajendar, A. Rajendran, Y. Sato, S. Nishizawa and N. Teramae, *Org. Biomol. Chem.*, 2009, **17**, 351; (*f*) B. Rajendar, A. Rajendran, Z. Ye, E. Kanai, Y. Sato, S. Nishizawa, M. Sikorski and N. Teramae, *Org. Biomol. Chem.*, 2010, **8**, 4949; (*g*) K. Benner, H. Ihmels, S. Kölsch and P. M. Pithan, *Org. Biomol. Chem.*, 2014, **12**, 1725.

25 D. V. Berdnikova, O. A. Fedorova, E. V. Tulyakova, H. Li, S. Kölsch and H. Ihmels, *Photochem. Photobiol.*, 2014, **91**, 723.

26 (*a*) M. M. Paquette, R. A. Kopelman, E. Beitler and N. L. Frank, *Chem. Commun.*, 2009, 5424; (*b*) W. Paw and R. Eisenberg, *Inorg. Chem.*, 1997, **36**, 2287; (*c*) J.-L. Pozzo, A. Samat, R. Guglielmetti and D. D. Keukeleire, *J. Chem. Soc., Perkin Trans. 2*, 1993, 1327.

27 A. Granzhan, H. Ihmels and G. Viola, *J. Am. Chem. Soc.*, 2007, **129**, 1254.